OXFORD

GENERAL & SELECTED POPULATIONS SECTION

Feasibility of Auricular Field Stimulation in Fibromyalgia: Evaluation by Functional Magnetic Resonance Imaging, Randomized Trial

Anna Woodbury (iD), MD*,[†] Venkatagiri Krishnamurthy, PhD*,[†] Melat Gebre, MD* Vitaly Napadow, PhD[‡]
Corinne Bicknese, MD* Mofei Liu, MSPH[§] Joshua Lukemire, MS[§] Jerry Kalangara, MD*,[†]
Xiangqin Cui, PhD,[†,§] Ying Guo, PhD[§] Roman Sniecinski, MD, MSCR* and Bruce Crosson, PhD*,[†]

*Emory University School of Medicine, Atlanta, Georgia; [†]Atlanta Veterans Affairs Health Care System, Atlanta, Georgia; [‡]Martinos Center for Biomedical Imaging, Massachusetts General Hospital, Harvard Medical School, Boston, Massachusetts; [§]Emory University Rollins School of Public Health, Atlanta, Georgia, USA

Correspondence to: Anna Woodbury, MD, Department of Anesthesiology, Emory University SOM, 1365 Clifton Road, Atlanta, GA 30322, USA. Tel: 404-778-5582; Fax: 404-686-4475; E-mail: anna.woodbury@va.gov, anna.woodbury@emory.edu.

Abstract

Objective. To evaluate the feasibility of recruitment, preliminary efficacy, and acceptability of auricular percutaneous electrical nerve field stimulation (PENFS) for the treatment of fibromyalgia in veterans, using neuroimaging as an outcome measure and a biomarker of treatment response. **Design.** Randomized, controlled, single-blind. **Setting.** Government hospital. **Subjects.** Twenty-one veterans with fibromyalgia were randomized to standard therapy (ST) control or ST with auricular PENFS treatment. **Methods.** Participants received weekly visits with a pain practitioner over 4 weeks. The PENFS group received reapplication of PENFS at each weekly visit. Resting-state functional connectivity magnetic resonance imaging (rs-fcMRI) data were collected within 2 weeks prior to initiating treatment and 2 weeks following the final treatment. Analysis of rs-fcMRI used a right posterior insula seed. Pain and function were assessed at baseline and at 2, 6, and 12 weeks post-treatment. **Results.** At 12 weeks post-treatment, there was a non-significant trend toward improved pain scores and significant improvements in pain interference with sleep among the PENFS treatment group as compared with the ST controls. Neuroimaging data displayed increased connectivity to areas of the cerebellum and executive control networks in the PENFS group as compared with the ST control group following treatment. **Conclusions.** There was a trend toward improved pain and function among veterans with fibromyalgia in the ST + PENFS group as compared with the ST control group. Pain and functional outcomes correlated with altered rs-fcMRI network connectivity. Neuroimaging results differed between groups, suggesting an alternative underlying mechanism for PENFS analgesia.

Key Words: Percutaneous Electrical Nerve Stimulation (PENS); Fibromyalgia; Alternative Therapies; Rehabilitation Medicine; Chronic Pain; Magnetic Resonance Imaging (MRI)

Introduction

Fibromyalgia is a chronic pain syndrome that consists of chronic widespread pain, decreased physical function, fatigue, psychoemotional and sleep disturbances, and various somatic complaints and affects approximately 8 million people in the United States [1]. It is estimated that fibromyalgia costs the US population over $20 billion per year in lost wages and disability [2, 3]. In Gulf War–Era veterans, the incidence of fibromyalgia is significantly higher in deployed personnel, making the veteran population a unique group in which to study fibromyalgia and its treatments [4]. Although the pathophysiologic mechanisms leading to development of the disease are not well established, there is sufficient evidence to support the idea that fibromyalgia is a disorder of autonomic nervous system dysfunction [5] and central (brain and spinal cord) pain-processing mechanisms [6]. One nonpharmacologic method for modulating autonomic nervous system dysregulation and treating pain is vagal nerve stimulation (VNS), which can be performed using the ear [7, 8]. The neuro-stim system (NSS) is a device approved by the Food and Drug Administration (FDA) for pain that targets the auricular branches of several cranial nerves, including the vagus via percutaneous electrical neural field stimulation (PENFS) [9, 10], providing a nonpharmacologic alternative for pain treatment.

Chronic, clinical pain is more difficult to study than experimental, evoked pain due to daily symptom fluctuations and lack of a controlled environment. Resting-state functional connectivity magnetic resonance imaging (rs-fcMRI) is a specific type of neuroimaging that has evolved as an objective tool with the potential to reduce some of the variability in measuring parameters in chronic pain. It is capable of indexing functional connectivity between specific brain areas in patients with chronic pain and reflects changes that occur during their treatment [11]. This imaging approach has also been used to develop biomarkers for clinical pain intensity [12]. In a study of 17 participants with fibromyalgia, changes were found in insular connectivity to the default mode network (DMN) that correlated with changes in pain scores following treatment [13]. Based on this prior work, we aimed to assess a similar number of participants for this feasibility study using a novel nonpharmacologic treatment for fibromyalgia: auricular PENFS.

We hypothesized that PENFS results in greater pain and functional improvements than standard therapy (ST) and that these improvements can be correlated with altered brain connectivity as evaluated by rs-fcMRI. To test this hypothesis, we conducted a feasibility study in which we randomized veterans with fibromyalgia (2010 American College of Rheumatology criteria) [14] to ST control or ST with PENFS and evaluated post-treatment changes in pain, function, and rs-fcMRI.

Methods

Study Procedure

We conducted an open-label, randomized, controlled trial. Study participants were prescreened using a chart review of patients at the Atlanta Veterans Affairs Health Care System and then were invited via a phone call for a face-to-face screening session to determine if they met the inclusion criteria. Baseline assessments and rs-fcMRI were obtained by a blinded investigator prior to initiation of the intervention. Participants were re-assessed at 2, 6, and 12 weeks post-treatment. Follow-up rs-fcMRI was also obtained at 2 weeks post-treatment to assess changes in connectivity.

Participants

Twenty-one adult male and female veterans with a diagnosis of fibromyalgia were block randomized and stratified by sex to ST or PENFS in addition to ST. The inclusion criteria were as follows:

Age, 20–60 years (limit set to minimize brain structural changes due to aging).
Diagnosis of fibromyalgia by the American College of Rheumatology 2010 criteria [15].
Right-handedness (to provide consistency in brain structure and function).
Pain score of 4 or greater on the Defense and Veterans Pain Rating Scale (DVPRS) in the 3 months prior to enrollment.
Intact skin in area of PENFS treatment.
Ability to safely tolerate MRI.

The exclusion criteria were as follows:

Pregnancy.
History of seizures or neurologic conditions that alter the brain.
Claustrophobia, MRI-incompatible implants, or other conditions incompatible with MRI.
History of uncontrolled psychiatric illness, autoimmune disease that leads to pain, or skin conditions that can increase risk of infection at the PENFS site.

All participants provided written informed consent approved by the Institutional Review Board of Emory University and the Veterans Affairs Research & Development Committee.

Assessments of Pain and Function

Participants who met the study criteria returned for baseline assessments, including rs-fcMRI, collection of biobehavioral information, arm curl, 30-second chair stand, DVPRS, and documented baseline analgesic consumption. Arm curl tests measured the total number of bicep curls a veteran could do on the left and right arms in 30 seconds (5-lb weight for women; 8-lb weight for men). The 30-second chair stand test measured the total number of full sit-to-stands a veteran could do in 30 seconds. The DVPRS is a validated measure of pain for military and veteran populations and includes pain interference questions in the realms of "activity," "sleep," "mood," and "stress" [16]. Participants were

asked to evaluate on a scale of 0 to 10 the level of their pain and the level to which pain interfered with their "activity," "sleep," "mood," and "stress," with 0 representing no pain or interference and 10 representing the worst pain.

Intervention

Participants were stratified based on sex and block randomized to either ST or ST plus PENFS using the NSS device. PENFS treatment consisted of a series of four weekly treatments as described in the following section. Participants were assessed for changes in pain and function at 2, 6, and 12 weeks post-treatment.

Patients randomized to PENFS had the NSS (Innovative Health Solutions, Versailles, IN) applied; a battery pack (external auricular device) was secured via adhesive to the back of the ear to provide continuous stimulation at preprogrammed frequencies and intensities through electrodes that were sterilely, percutaneously placed at neurovascular bundles. The device was placed in the clinic, and the participants wore the device home continually until it was replaced at each weekly visit over 4 weeks. The external auricular device of the NSS is an FDA-cleared neuromodulating generator targeting acute and chronic pain with a frequency of 1–10 Hz, a pulse width of 1 millisecond, an amplitude of 3.2 V, an impulse of 100 mW, a length of stimulation of 120 hours, and a duty cycle of 2 hours on and 2 hours off.

All PENFS electrode placement points were located through transillumination, with one grounding electrode applied to the posterior concha and three electrode points to stimulate the respective auricular nerve endings (greater auricular, auricular branch of vagus, and auriculotemporal; Figure 1). The NSS uses a needle array instead of a single pin to help provide a field effect. Due to the effects of "field stimulation," the external auricle and its cranial nerve branches, including the vagal branch, receive stimulation [9].

ST consisted of medication management with neuropathic pain medications (gabapentin, pregabalin, duloxetine, tricyclic antidepressants, and so on), nonsteroidal anti-inflammatory medications (ibuprofen, meloxicam, and so on), topicals (lidocaine/prilocaine cream, menthol/salicylate, and so on), muscle relaxants (tizanidine, cyclobenzaprine, baclofen, and so on), and referral to acupuncture and physical therapy, tailored to the individual patient based on comorbid conditions and patient preference. Patients were evaluated weekly over 4 weeks in parallel to the weekly interventions performed on the PENFS treatment group.

MRI Acquisition

Blood oxygen level–dependent (BOLD) rs-fcMRI images were acquired on a 3 T Siemens Trio 3 T MRI scanner with a 32-channel phased-array head coil using a single-
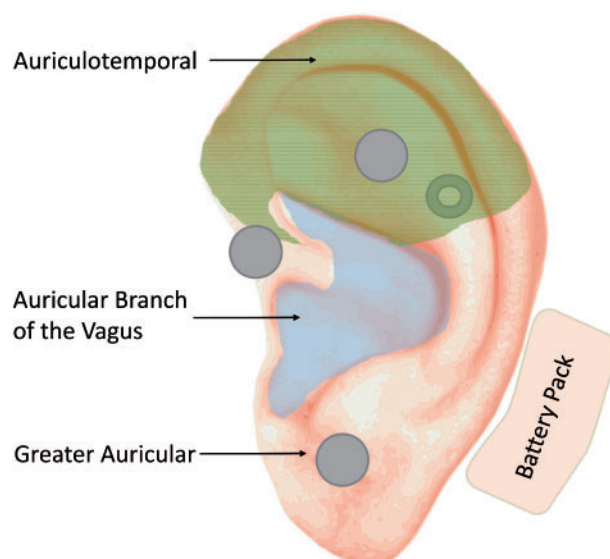

Figure 1. Depiction of the auricle showing nerve distributions and sample NSS placement. Electrode placement is shown using gray dots. The gray donut depicts one electrode array placed on the posterior pinna. Wire harnesses are not depicted. The battery pack is depicted with its usual placement posterior to the auricle.

shot gradient-echo echo planar imaging (EPI) sequence with the following MRI parameters:

Field of view (FOV) of 220 mm.
Repetition time/echo time (TR/TE) of 2,000/25 milliseconds
Multiband acceleration factor of 3.
Flip angle (FA) of 60°.
Matrix size of 110 × 110.
Slice thickness of 2 mm.
Generalized autocalibrating partial parallel acquisition (GRAPPA) factor of 2.
Partial Fourier of 6/8.
Thirty-four phase-encoded reference lines.
Seventy-two interleaved axial slices covering the entire brain. Three hundred fifty scan volumes to yield 9 minutes of resting-state fMRI data for stable estimation of connectivity networks.

A 1-mm^3 isotropic high-resolution T1-weighted anatomical image for spatial normalization to Montreal Neurological Institute (MNI) template space was acquired using a magnetization-prepared rapid gradient echo (MPRAGE) sequence with the following parameters: TE of 2.89 milliseconds, TR of 2,300 milliseconds, FOV of 256 mm^2 × 256 mm^2, FA of 8°, and matrix size of 256 × 256. To correct for EPI geometric distortions, a pair of spin echo EPI scans with opposite phase-encoding directions ("top up") [17] were acquired that were designed with the same echo spacing and bandwidth as the task fMRI (echo spacing [ES] of 0.69 milliseconds and bandwidth [BW] of 2,272 Hz/px). The participant's head was comfortably stabilized using foam pads to minimize motion during and between scans.

Image Processing

The BOLD EPI images were processed systematically with a combination of Analysis of Functional Neuro-Images (AFNI), FMRIB Software Library (FSL), and Matlab (Natick, MA) in-house scripts [18, 19]. To systematically delineate the clinical intervention-based connectivity changes, we used a highly validated and optimized rs-fcMRI pipeline developed by our group [20] tailored to pain studies [13, 21–23]. The rs-fcMRI volumes were corrected for slice timing, bulk head motion, and EPI distortion [17]. In parallel, the T1-weighted MPRAGE images were skull stripped using Optimized Brain Extraction Tool (optiBET) [24] and spatially transformed to an MNI-152 standard template using FSL's linear (FLIRT) and nonlinear (FNIRT) spatial transformation algorithms. The EPI distortion–corrected rs-fcMRI images were then de-noised for various artifacts (such as cardiac and respiratory, hardware, susceptibility and motion artifacts) using standard FSL tools (FIX) that employ independent component analysis (ICA)–based de-noising methodologies. The de-noised images were then co-registered with the T1-weighted MPRAGE using FSL's boundary-based registration algorithm (epi_reg) and then warped to MNI space using the MPRAGE-to-MNI transformation warp images. To reduce influence from cerebrospinal fluid pulsatility and resulting partial volume effects near the edge of the ventricles, we masked the ventricles in the rs-fcMRI time course. We then temporally filtered the rs-fcMRI time course using a Chebyshev II low-pass filter cutoff frequency of 0.32 Hz, and then the signal intensity across neighboring voxels for each volume was spatially smoothed using a Gaussian filter full width at half maximum (FWHM) of 4 mm. From the motion parameters captured during the global head motion correction, frame-to-frame displacement was computed [25], and time points from the rs-fcMRI time series were censored at a threshold of 0.3 mm. For whole-brain connectivity analyses using a seed-based approach, a sphere (5-mm radius) centered at the seed MNI coordinates was used to generate an average seed time course to cross-correlate with the time courses of all other voxels [26]. The Fisher z transform was applied to the cross-correlation values to normalize the distribution.

Statistical Analysis

Analysis of sample characteristics for the groups was conducted to assess comparability of the samples. Categorical variables such as sex and biobehavioral data were assessed using Fisher's exact test, but continuous variables such as age were assessed using two-tailed t tests. All reported P values are two tailed and considered significant at the 0.05 level, family-wise error (FWE) corrected. To quantify brain connectivity, rs-fcMRI data were analyzed with both a seed-voxel and pairwise connectivity via the partial correlations approach [25].

Primary Outcome (rs-fcMRI as a Biomarker of Treatment Outcomes)

Seed-Voxel Functional Connectivity Approach. Prior studies regarding fibromyalgia and pain have identified altered network connectivity using seeds in the inferior parietal lobule (IPL), right dorsolateral prefrontal cortex (R-dlPFC), dorsal anterior cingulate cortex (dACC), insula, right temporoparietal junction (R-TPJ), medial prefrontal cortex (mPFC), and sensorimotor network (SMN) [11, 21, 23, 27–31]. These areas were carefully chosen to avoid extending into white matter, into cerebrospinal fluid, or outside the brain. Based on this existing data, seed-based resting connectivity analyses between relevant areas were performed. The seeds were spherical, 1 cm in diameter, and centered on the MNI peak coordinates of regions of activity defined from prior published studies [11, 21, 23, 27–31]. The same seeds were eroded to include only gray-matter voxels using the Johns Hopkins University International Consortium of Brain Mapping white-matter atlas [32]. We then correlated the averaged time series from the seed regions using AFNI.

Connectivity Analysis via Partial Correlations. To evaluate the feasibility of using fcMRI as a biomarker in PENFS treatment outcomes, we evaluated the association between the participants' DVPRS scores and brain connectivity (using partial correlations) and tested for significance. Following the aforementioned processing steps, we used correlation coefficients to investigate the association between the baseline resting SMN–DMN connectivity and post-PENFS changes in pain levels. Pairwise connectivity between node pairs was assessed via partial correlation. Partial correlation has shown great promise in accurately detecting true brain network connections measuring the direct connectivity between two nodes and avoiding spurious effects in network modeling [33]. We estimated partial correlations using *DensParCorr*, a statistical R package that implements an efficient and reliable statistical method for estimating partial correlation in large-scale brain network modeling [34]. To examine the relationship between brain connectivity (via partial correlation) and DVPRS scores, we first obtained the partial correlation connectivity matrix using the *DensParCorr* package for each participant. Then, for each pair of regions of interest (ROIs), we calculated the correlation between the participants' connectivity and DVPRS scores to assess their association.

Secondary Outcome (Improvements in Clinical Pain and Function)

Participants were measured at baseline, 2 weeks, 6 weeks, and 12 weeks. Mixed-effect linear regression was used to model each outcome separately. The model predictors included treatments (treatment vs control), time (the four time points), and the interaction of treatment and time,

Table 1. Demographic and medical characteristics of study population

Characteristics	PENFS Treatment (n = 12)	Standard Therapy Control (n = 9)	P Value
Age, mean years	50 ± 9.78	48.56 ± 10.08	0.68
Gender			
Female	6 (50%)	6 (67%)	0.47
Male	6 (50%)	3 (33%)	—
Race			
Caucasian	7 (58%)	4 (44%)	0.55
African American	5 (42%)	5 (56%)	—
Ethnicity			
Hispanic	1 (9%)	1 (11%)	0.84
Non-Hispanic	10 (83%)	8 (89%)	—
Unknown	1 (8%)	0 (0%)	—
Baseline pain scores, mean DVPRS	6.42 ± 1.64	8 ± 1.52	0.04*
Baseline sit-to-stand	8.67 ± 4.48	6.44 ± 3.21	0.22
Baseline bicep curls			
Left	18.92 ± 7.20	15.33 ± 7.66	0.29
Right	18.58 ± 6.51	14.89 ± 7.27	0.24

PENFS = percutaneous electrical nerve field stimulation; DVPRS = Defense and Veterans Pain Rating Scale.
*$P<0.05$. Means are reported with 95% confidence intervals (mean ± 1.96 standard deviation).

Table 2. Change in pain score (Defense and Veterans Pain Rating Scale [DVPRS]) and function following therapy

Time Point	Total Cohort	Outcome Variable	Treatment (PENFS)	Control (Standard Therapy)	P Value
2 weeks	16 (9 PENFS)	DVPRS	–0.9 ± 3.5	–1.4 ± 7.4	0.80
		Sit-to-stand	2.7 ± 6.6	0.3 ± 8.1	0.24
		Bicep curls (left)	4.6 ± 12.7	1.7 ± 13.7	0.42
		Bicep curls (right)	4.2 ± 10.0	0.7 ± 15.1	0.32
6 weeks	14 (8 PENFS)	DVPRS	–1.1 ± 4.0	–0.5 ± 2.1	0.52
		Sit-to-stand	3.1 ± 9.7	0.3 ± 8.1	0.27
		Bicep curls (left)	6.1 ± 13.1	–1.8 ± 12.4	0.04*
		Bicep curls (right)	6.0 ± 14.4	0.8 ± 13.2	0.2
12 weeks	14 (9 PENFS)	DVPRS	–1.3 ± 4.0	–0.1 ± 3.3	0.27
		Sit-to-stand	1.7 ± 8.7	1.4 ± 7.7	0.91
		Bicep curls (left)	5.8 ± 13.2	0.0 ± 15.5	0.21
		Bicep curls (right)	4.6 ± 13.3	0.2 ± 11.4	0.24

PENFS = percutaneous electrical nerve field stimulation.
*$P<0.05$. Means are reported with 95% confidence intervals (mean ± 1.96 standard deviation).

with subject as a random effect. The significance level was set at 0.05. Data analysis was conducted with R version 3.6.3 on the RStudio platform. The ggplot2 package was used to generate trend plots, and the lmerTest package was used to fit the mixed-effect linear regression model.

Results

A total of 21 participants were block randomized to either PENFS treatment or ST control (ST; n=9) or ST with auricular PENFS (ST + PENFS; n=12). Baseline demographic characteristics such as age, gender, race, and ethnicity did not significantly differ between the groups. However, due to the small sample size, and as a product of chance randomization, study participants assigned to the PENFS treatment group had significantly lower pain scores at baseline than the ST control group (Table 1).

Two participants complained of minor irritation at the site with PENFS treatment. No major adverse events were reported. All participants randomized to the PENFS treatment group completed both imaging evaluations and the 4-week and 12-week follow-up visits in addition to the baseline visits. However, we excluded three PENFS treatment participants from analysis; two participants experienced extenuating circumstances (cervical disc herniation and loss of home) during the study period; the third participant received an fMRI that could not be adequately processed due to anatomical variations in the participant's brain, unrelated to exclusion criteria. Two participants in the ST control group did not present for their follow-up fMRI. Therefore, these individuals were excluded from analysis, leaving us with a total cohort of nine PENFS treatment participants and seven ST control participants for analysis. Not all individuals presented for all follow-up visits, but all participants included in
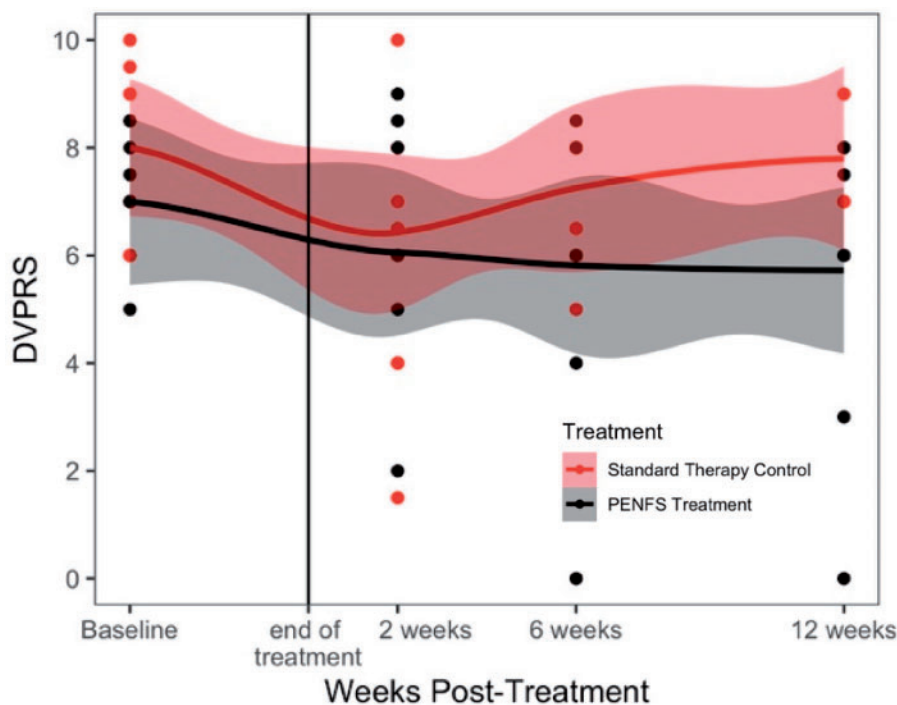
Figure 2. Pain scores over time in PENFS treatment and standard therapy control groups. Participants were assessed at baseline, and at 2, 6, and 12 weeks following the 4-week intervention (PENFS treatment + standard therapy vs. standard therapy control). Individual subjects are represented by dots, some of which overlap. The confidence intervals are shown in shading around each mean, which is represented by a solid line. All pain measures were obtained using the Defense and Veterans Pain Rating Scale (DVPRS). There was a trend towards improved pain scores in the PENFS treatment group as compared to the standard therapy control group at 12 weeks post-treatment.

Table 3. Change in pain interference scores related to activity, sleep, mood, and stress following therapy

Time Point	Total Cohort	Outcome Variable	Treatment (PENFS)	Control (Standard Therapy)	P Value
2 weeks	16 (9 PENFS)	Activity	–1.2 ± 3.5	0.9 ± 8.9	0.3
		Sleep	–1.6 ± 5.8	–0.4 ± 11.3	0.63
		Mood	–1.0 ± 5.1	–0.6 ± 10.5	0.85
		Stress	–1.4 ± 3.6	0.0 ± 9.7	0.5
6 weeks	14 (8 PENFS)	Activity	–1.2 ± 4.5	1.2 ± 3.1	0.04*
		Sleep	–1.6 ± 5.5	1.8 ± 4.2	0.02*
		Mood	–1.4 ± 5.3	1.8 ± 4.5	0.03*
		Stress	–1.8 ± 4.4	1.7 ± 3.6	0.01*
12 weeks	14 (9 PENFS)	Activity	–1.6 ± 4.7	1.0 ± 7.2	0.2
		Sleep	–1.7 ± 4.6	2.2 ± 5.9	0.04*
		Mood	–2.1 ± 4.3	1.8 ± 7.3	0.08
		Stress	–1.9 ± 3.3	1.8 ± 6.4	0.06

PENFS = percutaneous electrical nerve field stimulation.

*P values less than 0.05 are considered statistically significant. Means are reported with 95% confidence intervals (mean ± 1.96 standard deviation).

the analysis were present for baseline assessments, pre-imaging and postimaging studies, and at least one follow-up visit. Missing data were not imputed and were not used for analysis to avoid distortions related to imputation in the small sample size. There were no significant differences in pain scores between the treatment or control group over time (Table 2). The PENFS treatment group displayed significant improvements in left-sided bicep curls as compared with the ST control group at 8 weeks following therapy (P=0.04); no other statistically significant differences were noted.

Although no significant differences were found in the pain scores between the two groups following treatment, there was a trend toward continued pain relief in the PENFS treatment group as opposed to the ST control group at 6 weeks and 12 weeks following treatment, whereas the ST control group appeared to return to baseline at 12 weeks (Figure 2). Outcomes related to function tended to improve in both groups following treatment, with similar results by week 12.

No statistically significant difference was found between groups at 2 weeks immediately following

treatment. At 6 weeks, participants in the PENFS group reported significantly improved pain interference with activity, sleep, and mood compared with participants who received ST alone (Table 3). At 12 weeks, participants in the PENFS group continued to report significant improvements in pain interference with sleep as compared with the ST group, although the effects on activity,

Table 4. Decreased connectivity following standard therapy (control group, right posterior insula seed)

Brain Region	Cluster Size (No. of Voxels)	Voxel (x, y, z)
Lobule VIII of cerebellum (L)	170	–38, –60, –52
Inferior parietal lobule (L)	111	–46, –54, 34
Crus II of cerebellum (L)	87	–12, –82, –42
Crus II of cerebellum (R)	78	50, –46, –42
Putamen (L)	78	–28, 8, 6
Posterior cingulate cortex (L)	61	–12, –44, 24
Lobule VIII of cerebellum (R)	47	26, –60, –46

L = left; R = right.

Coordinates are reported in Montreal Neurological Institute (MNI) space (mm), and regions are grouped according to the cluster to which they belong. All regions were located based on connectivity to the right posterior insula seed and reflected decreased connectivity ($P=0.05$). Regions are listed in order of descending cluster size.

Table 5. Increased connectivity following percutaneous electrical nerve field stimulation (PENFS) treatment (PENFS group, right posterior insula seed)

Brain Region	Cluster Size (No. of Voxels)	Voxel (x, y, z)
Middle occipital gyrus (R)	170	42, –88, 0
Midbrain (L)	71	–8, –32, –10
Anterior insula (L)	58	–36, 14, –16
Lobule IX of cerebellum (R)	41	2, –56, –58

R = right; L = left.

Coordinates are reported in Montreal Neurological Institute (MNI) space (mm), and regions are grouped according to the cluster to which they belong. All regions were located based on connectivity to the right posterior insula seed and reflected increased connectivity ($P=0.05$).

mood, and stress diminished. Additional graphs of outcomes from Table 2 and Table 3 can be found in the Supplementary Data.

Neuroimaging outcomes were analyzed using seed-voxel analysis based on a priori hypotheses with a carefully selected group of seeds implicated in pain and emotional regulation. With conservative motion scrubbing, as described in the *Methods* section, an average of $5.9\%\pm10.9\%$ of data was censored across all participants and all scans. The groups did not significantly differ in regard to motion, nor did motion significantly differ between baseline and follow-up within each group, and each participant had at least 4 minutes of data remaining after censoring, in alignment with the recent recommendations made by Parkes et al. [35]. In the ST control group, decreased connectivity (post-treatment vs pretreatment) was found from the right posterior insula to the bilateral lobule VIII of the cerebellum, left IPL, bilateral crus II of the cerebellum, left putamen, and left posterior cingulate cortex (PCC) following treatment (Table 4). This corresponds with decreased pain scores initially following treatment (Table 2).

In the PENFS treatment group, increased connectivity (post-treatment vs pretreatment) was found from the right posterior insula to the right middle occipital gyrus, left midbrain, left anterior insula, and right lobule IX of the cerebellum following treatment (Table 5). This corresponded with decreased pain scores initially following treatment (Table 2).

Using a right posterior insula seed, a difference of the differences (post-treatment vs pretreatment for treatment vs control) was measured, reflecting increased connectivity in the PENFS group as compared with the control group to areas associated with descending modulation of pain (Table 6; Figure 3). Decreased connectivity was found in the PENFS group as compared with the control group from the right posterior insula to the right IPL, an area of the DMN (Table 6). We must emphasize that this is a difference of change scores; thus, the baseline rs-

Table 6. Between-group differences in connectivity following treatment

Brain Region	Cluster Size (No. of Voxels)	Voxel (x, y, z)	Direction of Change (PENFS vs Control)
Lobule VII of cerebellum (R)	203	44, –50, –42	Increased
Lobule VII of cerebellum (L)	200	–38, –60, –52	Increased
Inferior frontal gyrus (L)	197	–58, 26, 8	Increased
Superior frontal sulcus (R)	188	24, 14, 42	Increased
Middle temporal gyrus (R)	164	58, 0, –28	Increased
Putamen (L)	150	–28, 8, 8	Increased
Superior frontal gyrus (L)	115	–28, 68, 6	Increased
Anterior cingulate (L)	108	–18, 44, –2	Increased
Brain stem (L)	77	–6, –32, –6	Increased
Inferior parietal lobule (R)	42	56, –42, 56	Decreased

PENFS = percutaneous electrical nerve field stimulation; R = right; L = left.

These connectivity measures are the result of a difference of differences (post-treatment vs pretreatment for PENFS minus post-treatment vs pretreatment for standard therapy control). Coordinates are reported in Montreal Neurological Institute (MNI) space (mm), and regions are grouped according to the cluster to which they belong. All regions were located based on connectivity to the right posterior insula seed ($P=0.05$).
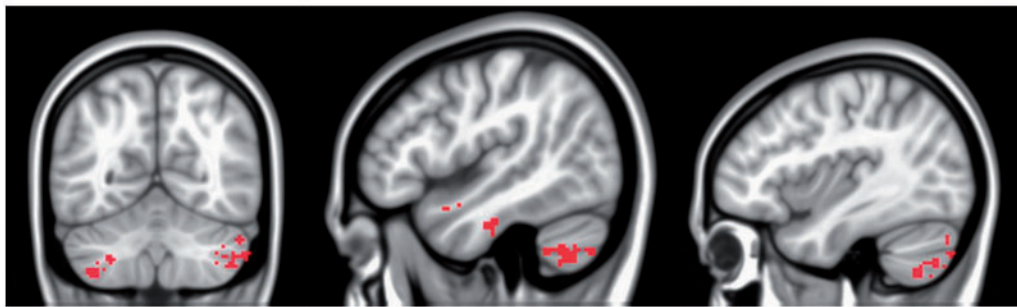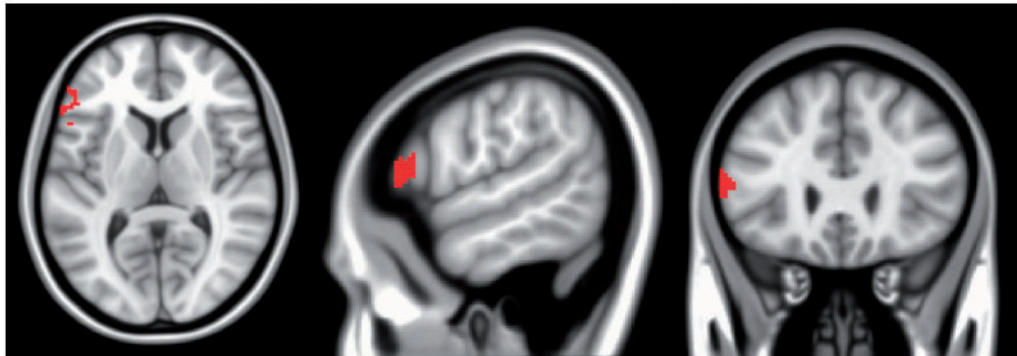
Left Cerebellum Lobule VIIB/Crus II and Right Cerebellum Lobule VIIB/Crus I-II

Left Inferior Frontal Gyrus

Right Superior Frontal Sulcus

Figure 3. Changes in Connectivity for PENFS Treatment Group Relative to Standard Therapy Control Group: Right Posterior Insula Seed. Seed-based analysis was performed using a right posterior insula seed, and changes in the standard therapy group (post-pre) were subtracted from changes in the PENFS group (post-pre). These changes were then analyzed using a 3 dimensional T-test. The PENFS group exhibited changes in connectivity (P=0.05) between the right posterior insula seed and areas depicted. Increased connectivity was found to bilateral cerebellar areas (left cerebellum lobule VIIB/Crus II and right cerebellum lobule VIIB/Crus I-II) post-treatment compared to the standard therapy control group. Other areas displaying increased connectivity included the left inferior frontal gyrus, right superior frontal sulcus, middle temporal gyrus, left putamen, left anterior cingulate cortex, and left brainstem. Decreased connectivity was found to the right inferior parietal lobule. These changes in connectivity reflect a comparison of between (intra-) group changes following treatment.

fcMRI was subtracted from the post-treatment rs-fcMRI for both groups, and then the difference from the ST control group was subtracted from the difference from the PENFS treatment group, resulting in the absolute differences found in Table 6.

Figure 3 highlights the difference of differences between the results of treatment for the PENFS group as compared with the ST control group using a right posterior insula seed. The figure reflects the increased connectivity from the right posterior insula to areas of the cerebellum implicated in pain and emotional regulation, as well as changes in connectivity to other areas involved in the descending modulation of pain.

Table 7 presents statistically significant correlations between post-treatment changes in DVPRS pain scores and brain connectivity measured by partial correlations between ROIs. Although the sample size is too small for multiple comparisons to be feasible, the effect sizes
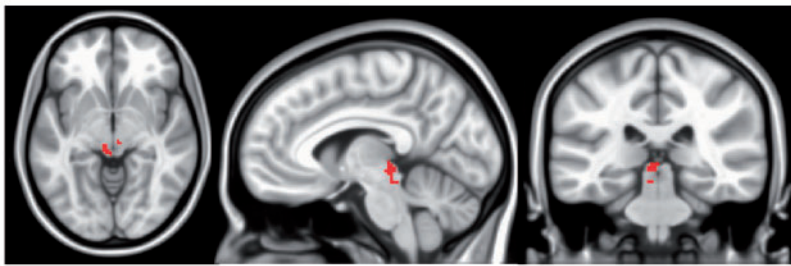
Middle Temporal Gyrus
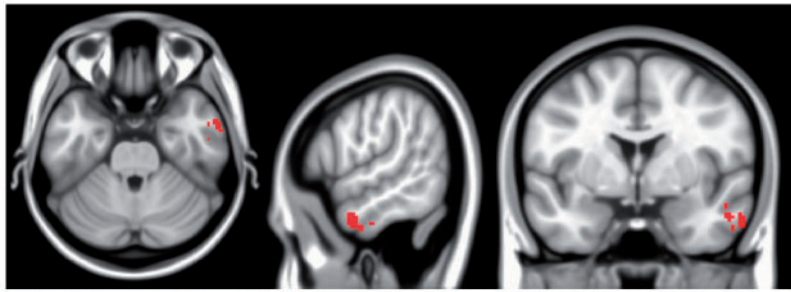
Left Putamen
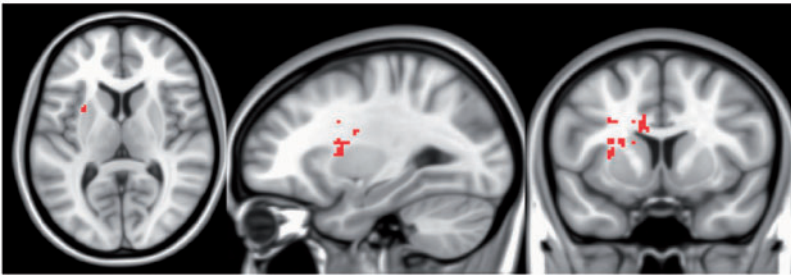
Left Anterior Cingulate Cortex

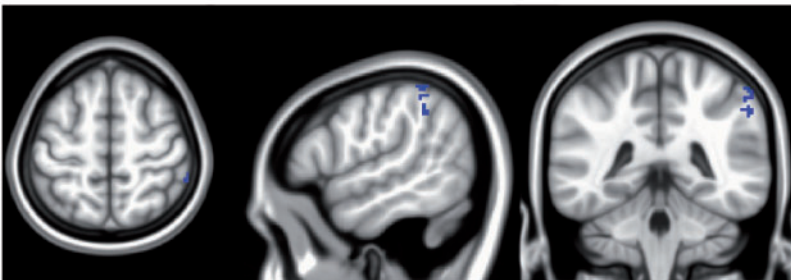Left Brainstem

Right Inferior Parietal Lobule

Figure 3. Continued.

Table 7. Connectivity between regions of interest (ROIs) statistically significantly correlated with Defense and Veterans Pain Rating Scale (DVPRS) scores

ROI 1	ROI 2	Correlation Between Brain Connectivity and DVPRS Scores	P Value
Right posterior insula	Left posterior insula	0.46	0.009*
Left posterior insula	Dorsal anterior cingulate cortex	0.364	0.044*
Left posterior insula	Left cerebellar lobule VI	−0.398	0.027*
Right dorsolateral prefrontal cortex	Left posterior cingulate cortex	0.421	0.018*
Right putamen	Right posterior cingulate cortex	0.383	0.034*
Left sensorimotor cortex I	Left cerebellar lobule VI	−0.483	0.006*
Medial prefrontal cortex	Left cerebellar lobule VI	0.408	0.023*

*$P<0.05$. All reported correlations exhibit effect sizes of medium strength or higher. Further details can be found in the corresponding heat map.

of the significant correlations reported are all medium or higher [36, 37]. A decrease in connectivity between the right posterior insula and left posterior insula was significantly associated with a decrease in DVPRS pain scores. Similarly, a decrease in connectivity between the left posterior insula and the dorsal anterior cingulate cortex (dACC) was associated with a decrease in DVPRS pain scores. Decreased connectivity from the right dorsolateral prefrontal cortex (dlPFC) to the left PCC was associated with a decrease in DVPRS pain scores. Decreased connectivity from the right putamen to the right PCC was associated with a decrease in DVPRS pain scores. Decreased connectivity between the medial prefrontal cortex (mPFC) and lobule VI of the left cerebellum was associated with a decrease in DVPRS pain scores. However, increased connectivity from the left sensorimotor cortex (S1M1) to lobule VI of the left cerebellum was associated with a decrease in DVPRS pain scores, and increased connectivity between the left posterior insula and lobule VI of the left cerebellum was associated with a decrease in DVPRS pain scores (Table 7). Supplementary Data depict a heat map of partial correlations between DVPRS and connectivity between selected ROIs implicated in pain and fibromyalgia. A heat map of *P* values is also shown.

Discussion

In our open-label neuroimaging feasibility study of 21 veterans with fibromyalgia who were randomized to either ST or ST with PENFS treatment, results reveal a trend toward improved pain and function in the PENFS group, along with meaningful changes in resting-state functional connectivity in pain-related areas. Participants who received PENFS reported significant ($P<0.05$) long-term (12 weeks) improvements in pain interference with sleep as compared with ST alone and significant improvements in function (left bicep curl) and all pain interference measures at 6 weeks. Other outcomes related to pain and function revealed a trend toward long-term improvement for the PENFS group over the ST group, although this was not statistically significant.

It was exciting to note that PENFS-related improvements in pain scores were present even at 12 weeks following the completion of treatment and correlated to changes in inter-network connectivity (i.e., salience network [SN], SMN, and DMN), which differed between groups. This suggests that PENFS may promote neuromodulation across brain areas and networks, resulting in neuroplasticity and longer-term pain relief following an initial input through a separate mechanism from ST, perhaps through VNS-induced neural plasticity, as reflected by changes on rs-fcMRI [38].

Results of our ST control group (Table 4) are consistent with results of prior studies evaluating rs-fcMRI in fibromyalgia, reflecting a decrease in connectivity between the insula and areas of the DMN associated with decreasing pain scores [11, 13, 29]. In contrast, the PENFS treatment group exhibited increased connectivity between the right posterior insula seed and the right middle occipital gyrus, left midbrain, left anterior insula, and right lobule IX of the cerebellum following treatment associated with decreased pain scores (Table 5), suggesting a different mechanism of action for PENFS-related treatment effects as compared with ST. These areas may provide new targets for neuromodulatory interventions in future studies of pain treatment, and their role in pain modulation requires further exploration. The difference of differences between the two groups (post-treatment vs pretreatment for the PENFS group vs the ST group) suggests modulation of the executive control network in relation to the cerebellum for the PENFS group as compared with the ST control group (Table 6). The executive control network (or frontoparietal control network) includes the superior frontal gyrus/sulcus, inferior frontal gyrus, middle temporal gyrus, and IPL and is thought to contribute to goal-based, deliberate action [39]. The cerebellum is one of the most commonly implicated areas of the brain in relation to pain and emotional processing [40–43]. This suggests that PENFS may exert an effect on modulating the emotional and executive control centers related to pain processing and may, in this way, decrease the interference of pain in daily activities.

Separate from the seed-based approach to evaluate differences in functional connectivity within and between

groups, we also sought to evaluate the correlation of connectivity between ROIs and overall changes in DVPRS scores to build on the use of neuroimaging as an outcome measure for pain. A partial correlations approach designed for neuroimaging analysis was used to correlate changes in DVPRS scores with changes in connectivity between a priori–identified ROIs (Table 7). Statistically significant correlations between post-treatment changes in DVPRS pain scores and brain connectivity were found for both intra-network and inter-network connectivity for the salience network, the somatomotor network, and the DMN.

In our proof-of-principle study, despite the small sample size, it was exciting to see consistent results that corroborated prior studies as well as novel PENFS-related findings. Our study had several limitations in addition to small sample size: lack of participant and provider blinding and lack of a placebo control group may result in a placebo-related effect; baseline differences in pain scores as a result of randomization may bias results toward the null. ST treatment was heterogeneous to allow for tailored treatments based on patient comorbidities, side effects, and prior treatment failures, but this may have resulted in increased variability. Effects of smoothing in rs-fcMRI data may also result in overlap of certain ROIs, potentially decreasing the accuracy of the results. Multiple comparison correction is too stringent to be feasible for the pairwise connectivity association analysis due to the small sample size of the current study and the large number of pairs of connections. However, the effect sizes of the significant correlations reported (Table 7) are all medium or higher [36, 37], indicating the statistical and clinical relevance of the identified associations.

Although our data are suggestive of an initial neural input resulting in a possible long-term neuromodulatory effect, further investigation is warranted. Future work may include a randomized, double-blind, placebo-controlled trial involving sham vs true PENFS and the utilization of advanced analyses such as hierarchical ICA. The utilization of brain-stem imaging and heart rate variability data may also aid in determining whether PENFS is acting through modulation of the vagal nucleus or through a different mechanism. Given that clinical pain scores continued to decrease at 12 weeks' follow-up, subsequent studies should also aim to evaluate long-term rs-fcMRI neural changes, as our rs-fcMRI data only evaluated immediate post-treatment effects as compared with baseline.

Conclusions

Overall, the results of this small open-label feasibility trial suggest a potential positive effect of PENFS as compared with ST alone and provide questions for further research and hypothesis generation. The clinical efficacy of PENFS for fibromyalgia should be explored in a larger randomized, double-blind, placebo-controlled trial.

Neuroimaging outcomes should additionally be evaluated at later time points to evaluate the long-term neuromodulatory effects of PENFS.

Supplementary Data

Supplementary Data may be found online at http://pain-medicine.oxfordjournals.org.

References

1. Heidari F, Afshari M, Moosazadeh M. Prevalence of fibromyalgia in general population and patients, a systematic review and meta-analysis. Rheumatol Int 2017;37(9):1527–39.
2. Berger A, Sadosky A, Dukes EM, Edelsberg J, Zlateva G, Oster G. Patterns of healthcare utilization and cost in patients with newly diagnosed fibromyalgia. Am J Manag Care 2010;16(5 Suppl):S126–37.
3. Robinson RL, Birnbaum HG, Morley MA, Sisitsky T, Greenberg PE, Claxton AJ. Economic cost and epidemiological characteristics of patients with fibromyalgia claims. J Rheumatol 2003;30(6):1318–25.
4. Eisen SA, Kang HK, Murphy FM, et al. Gulf War veterans' health: Medical evaluation of a U.S. cohort. Ann Intern Med 2005;142(11):881–90.
5. Martinez-Lavin M, Hermosillo AG. Dysautonomia in Gulf War syndrome and in fibromyalgia. Am J Med 2005;118(4):446.
6. Petersel DL, Dror V, Cheung R. Central amplification and fibromyalgia: Disorder of pain processing. J Neurosci Res 2011;89 (1):29–34.
7. Chakravarthy K, Chaudhry H, Williams K, Christo PJ. Review of the uses of vagal nerve stimulation in chronic pain management. Curr Pain Headache Rep 2015;19(12):54.
8. Napadow V, Edwards RR, Cahalan CM, et al. Evoked pain analgesia in chronic pelvic pain patients using respiratory-gated auricular vagal afferent nerve stimulation. Pain Med 2012;13 (6):777–89.
9. Fraser L, Woodbury A. Case report: Percutaneous electrical neural field stimulation in two cases of sympathetically-mediated pain. F1000Res 2017;6:920.
10. Gebre M, Woodbury A, Napadow V, et al. Functional magnetic resonance imaging evaluation of auricular percutaneous electrical neural field stimulation for fibromyalgia: Protocol for a feasibility study. JMIR Res Protoc 2018;7(2):e39.
11. Napadow V, Harris RE. What has functional connectivity and chemical neuroimaging in fibromyalgia taught us about the mechanisms and management of 'centralized' pain? Arthritis Res Ther 2014;16(5):425.

12. Lee J, Mawla I, Kim J, et al. Machine learning-based prediction of clinical pain using multimodal neuroimaging and autonomic metrics. Pain 2019;160(3):550–60.

13. Harris RE, Napadow V, Huggins JP, et al. Pregabalin rectifies aberrant brain chemistry, connectivity, and functional response in chronic pain patients. Anesthesiology 2013;119(6):1453–64.

14. Wolfe F, Clauw DJ, Fitzcharles MA, et al. The American College of Rheumatology preliminary diagnostic criteria for fibromyalgia and measurement of symptom severity. Arthritis Care Res (Hoboken) 2010;62(5):600–10.

15. Wolfe F, Clauw DJ, Fitzcharles MA, et al. 2016 revisions to the 2010/2011 fibromyalgia diagnostic criteria. Semin Arthritis Rheum 2016;46(3):319–29.

16. Buckenmaier CC 3rd, Galloway KT, Polomano RC, McDuffie M, Kwon N, Gallagher RM. Preliminary validation of the Defense and Veterans Pain Rating Scale (DVPRS) in a military population. Pain Med 2013;14(1):110–23.

17. Andersson JL, Skare S, Ashburner J. How to correct susceptibility distortions in spin-echo echo-planar images: Application to diffusion tensor imaging. Neuroimage 2003;20(2):870–88.

18. Cox RW. AFNI: Software for analysis and visualization of functional magnetic resonance neuroimages. Comput Biomed Res 1996;29(3):162–73.

19. Smith SM, Jenkinson M, Woolrich MW, Beckmann CF, et al. Advances in functional and structural MR image analysis and implementation as FSL. Neuroimage 2004;23(suppl 1):S208–19.

20. Krishnamurthy V, Krishnamurthy LC, Schwam DM, et al. Retrospective correction of physiological noise: Impact on sensitivity, specificity, and reproducibility of resting-state functional connectivity in a reading network model. Brain Connect 2018;8(2):94–105.

21. Puiu T, Kairys AE, Pauer L, et al. Association of alterations in gray matter volume with reduced evoked-pain connectivity following short-term administration of pregabalin in patients with fibromyalgia. Arthritis Rheumatol 2016;68(6):1511–21.

22. Zucker NA, Tsodikov A, Mist SD, Cina S, Napadow V, Harris RE. Evoked pressure pain sensitivity is associated with differential analgesic response to verum and sham acupuncture in fibromyalgia. Pain Med 2017;18(8):1582–92.

23. Hemington KS, Wu Q, Kucyi A, Inman RD, Davis KD. Abnormal cross-network functional connectivity in chronic pain and its association with clinical symptoms. Brain Struct Funct 2016;221(8):4203–19.

24. Lutkenhoff ES, Rosenberg M, Chiang J, et al. Optimized brain extraction for pathological brains (optiBET). PLoS One 2014;9 (12):e115551.

25. Power JD, Mitra A, Laumann TO, Snyder AZ, Schlaggar BL, Petersen SE. Methods to detect, characterize, and remove motion artifact in resting state fMRI. Neuroimage 2014;84:320–41.

26. Krishnamurthy V, Gopinath K, Brown GS, Hampstead BM. Resting-state fMRI reveals enhanced functional connectivity in spatial navigation networks after transcranial direct current stimulation. Neurosci Lett 2015;604:80–5.

27. Ichesco E, Schmidt-Wilcke T, Bhavsar R, et al. Altered resting state connectivity of the insular cortex in individuals with fibromyalgia. J Pain 2014;15(8):815–26.e1.

28. Kim J, Loggia ML, Cahalan CM, et al. The somatosensory link in fibromyalgia: Functional connectivity of the primary somatosensory cortex is altered by sustained pain and is associated with clinical/autonomic dysfunction. Arthritis Rheumatol 2015;67 (5):1395–405.

29. Napadow V, LaCount L, Park K, As-Sanie S, Clauw DJ, Harris RE. Intrinsic brain connectivity in fibromyalgia is associated with chronic pain intensity. Arthritis Rheum 2010;62(8):2545–55.

30. Napadow V, Kim J, Clauw DJ, Harris RE. Decreased intrinsic brain connectivity is associated with reduced clinical pain in fibromyalgia. Arthritis Rheum 2012;64(7):2398–403.

31. Cifre I, Sitges C, Fraiman D, et al. Disrupted functional connectivity of the pain network in fibromyalgia. Psychosom Med 2012;74(1):55–62.

32. Oishi K, Zilles K, Amunts K, et al. Human brain white matter atlas: Identification and assignment of common anatomical structures in superficial white matter. Neuroimage 2008;43(3):447–57.

33. Smith SM. The future of FMRI connectivity. Neuroimage 2012; 62(2):1257–66.

34. Wang Y, Kang J, Kemmer PB, Guo Y. An efficient and reliable statistical method for estimating functional connectivity in large scale brain networks using partial correlation. Front Neurosci 2016;10:123.

35. Parkes L, Fulcher B, Yücel M, Fornito A. An evaluation of the efficacy, reliability, and sensitivity of motion correction strategies for resting-state functional MRI. Neuroimage 2018;171 :415–36.

36. Cohen J. Statistical power analysis. Curr Dir Psychol Sci 1992;1 (3):98–101.

37. Cohen J. Statistical Power Analysis for the Behavioral Sciences. Abingdon, England: Routledge; 1988.

38. Hays SA, Rennaker RL, Kilgard MP. Targeting plasticity with vagus nerve stimulation to treat neurological disease. Prog Brain Res 2013;207:275–99.

39. Dixon ML, De La Vega A, Mills C, et al. Heterogeneity within the frontoparietal control network and its relationship to the default and dorsal attention networks. Proc Natl Acad Sci USA 2018;115(7):E1598–E607.

40. Strata P. The emotional cerebellum. Cerebellum 2015;14(5):570–7.

41. Michelle Welman FHS, Smit AE, Jongen JLM, Tibboel D, van der Geest JN, Holstege JC. Pain experience is somatotopically organized and overlaps with pain anticipation in the human cerebellum. Cerebellum 2018;17(4):447–60.

42. Coombes SA, Misra G. Pain and motor processing in the human cerebellum. Pain 2016;157(1):117–27.

43. Moulton EA, Schmahmann JD, Becerra L, Borsook D. The cerebellum and pain: Passive integrator or active participator? Brain Res Rev 2010;65(1):14–27.